revue en ligne : https://journals.openedition.org/geomorphologie/

Géomorphologie : Relief, Processus, Environnement

vol. 28, n° 4 (2022), p. xxx-xxx
Mise en ligne le 23 novembre 2022 sur journals.openedition.org
https://journals.openedition.org/geomorphologie/17247
DOI:10.4000/geomorphologie.17247

http://edytem.univ-savoie.fr/gfg/

Late Pleistocene-Holocene fluvial records of the Wadi Dishshah: hydro-climatic and archaeological implications (Southern piedmont of the Hajar Mountains, Oman)

Enregistrement fluviatile au Pléistocène supérieur et à l'Holocène du Wadi Dishshah (piémont sud du Jebel Hajar, Oman) : implications hydro-climatiques et archéologiques

Tara Beuzen-Waller [a*], Stéphane Desruelles [b], Anaïs Marrast [c], Jessica Giraud [d], Guillaume Gernez [d], Steven Forman [e], Amir Beshkani [f], Stéphanie Bonilauri [g], Marion Lemée [h], Hugo Nacarro [i], Eric Fouache [j]

[a] Soil science and Geomorphology Working Group, University of Tübingen - Eberhard Karls University Tübingen, Soil Science and Geomorphology, Rümelinstraße 19 – 23, 72070 Tübingen, Germany.
[b] UR Médiations - Sciences des lieux, sciences des liens, Sorbonne Abu Dhabi University, Jazeerat Al Reem, P.O. Box 38044, Abou Dhabi, United Arab Emirates.
[c] UMR AASPE 7209 - 43, rue Buffon - CP 56 Muséum national d'Histoire Naturelle, 75005 Paris, France.
[d] UMR 7041 – ArScAn – VEPMO, Maison de l'Archéologie et de l'Ethnologie 21 allée de l'Université F-92023 Nanterre, France.
[e] Geoluminescence Dating Research Laboratory, Institute of Archaeology, One Bear Place 97354, Baylor University, Waco,TX 76798, United States of America.
[f] UMR 7041 – ArScAn – AnTET, Maison de l'Archéologie et de l'Ethnologie 21 allée de l'Université F-92023 Nanterre, France.
[g] UMR 7194 HNHP – PRETROP, musée de l'Homme, 17 place du Trocadéro, 75116, Paris, France.
[h] INRAP - 37 Rue du Bignon, 35510 Cesson-Sévigné, France.
[i] UR Médiations - Sciences des lieux, sciences des liens, Sorbonne Université, 28 Rue Serpente, 75006 Paris, France.

ARTICLE INFORMATION
Received 28 march 2022.
Received in revised form 8 november 2022.
Accepted 17 october 2022.

*Corresponding author. Tel: +49 (0)7071 29 78939;
E-mail adresses:
tara.beuzen-waller@uni-tuebingen.de (Tara Beuzen-waller)
stephanedesruelles@gmail.com (Stéphane Desruelles)
anais.marrast@gmail.com (Anaïs Marrast)
giraud.jessica@gmail.com (Jessica Giraud)
Guillaume.Gernez@gmail.com (Guillaume Gernez)
Steven_Forman@baylor.edu (Steven Forman)
A.Beshkani@gmail.com (Amir Beshkani)
stephanie.bonilauri@mnhn.fr (Stéphanie Bonilauri)
lemeemarion@gmail.com (Marion Lemée)
Hugo.Naccaro@malix.univ-paris1.fr (Hugo Nacarro)
eric.fouache@sorbonne-universite.fr (Eric Fouache)

ABSTRACT

In Oman, quaternary climatic fluctuations alternated between humid and arid periods. Humid periods are a key component in landscape evolution and the history of early human-environment interactions, as they allowed for less-restrictive arid conditions by triggering increasing rainfall and fluvio-lacustrine activity. Fluvial archives are of great interest for understanding hydrosystems' local responses to quaternary regional climatic fluctuations. For the end of the Pleistocene and the Holocene, little data are available in Northern Oman to examine this topic and to compare it with archaeological site distribution and subsistence strategies, in particular with regard to water resources. Here, we will present fluvial records from a small wadi called Wadi Dishshah, located in the southern part of the Hajar Mountains' piedmont, near the Salakh Arch area. The study of the Wadi Dishshah relies on topographic surveys (aerial survey with drone), geomorphological mapping, morphostratigraphic analyses of natural and excavated sections, malacological analyses and age-dating using OSL and radiocarbon methods. Three phases of aggradation have been identified: the first one between 26,500 cal. BP and 11,300 cal. BP, a second between 6,200 cal. BP and 5,500 cal. BP and a late one around 2,800 cal. BP. The fluvial records from the Wadi Dishshah and its hydro-climatic significance are compared to the distribution of archaeological sites from the Salakh Arch area to discuss the relations between settlement strategies and surface flows. This work is the first case study of late Pleistocene – Holocene alluvial formations in this region of Oman.

Keywords: Fluvial archives; Pluvial periods; Geoarchaeology; Hajar Mountains; Oman.

RÉSUMÉ

À Oman, les fluctuations climatiques sont caractérisées par une alternance entre périodes humides et périodes arides. Les périodes humides sont des moments clés dans l'histoire des interactions hommes-milieux car elles occasionnent une augmentation significative de la pluviométrie. Pour étudier les réponses locales des hydrosystèmes aux fluctuations climatiques régionales, les archives fluviales sont des enregistrements appropriés. Cependant, les formations alluviales du Pléistocène supérieur et de l'Holocène sont encore peu étudiées, en particulier au Nord du Sultanat d'Oman où l'extrême rareté des données locales ne permet pas de comparer la chronologie climatique avec la distribution des sites archéologiques par périodes ou avec l'évolution des stratégies de subsistance. Dans cet article, nous présentons une étude inédite sur les formations alluviales héritées d'un petit wadi secondaire du piémont sud du Jebel Hajar : le Wadi Dishshah. A partir de la cartographie géomorphologique d'un tronçon, de l'étude morphostratigraphique de six coupes, de leurs datations par OSL et par radiocarbone et d'une étude malacologique effectuée sur une coupe, trois générations de dépôts alluviaux sont identifiées. La première génération de dépôts est datée entre 26 500 cal. BP et 11 300 cal. BP, la deuxième génération entre 6 200 cal. BP et 5 500 cal. BP et une dernière phase d'accumulation est datée à environ 2 800 cal. BP. Leur signification hydro-climatique est discutée et comparée avec la distribution des sites archéologiques préhistoriques et protohistoriques préalablement découverts dans ce secteur.

Mots-clés : *Archives fluviales ; Périodes humides ; Géoarchéologie ; Jebel Hajar ; Oman.*

1. Introduction

1.1. Quaternary climatic fluctuations in Oman: between arid and humid periods

In Arabia, Quaternary climate is controlled by rainfall variations and alternate between arid and humid periods, mainly linked to migration of the Intertropical Convergence Zone (ITCZ) and the monsoon rainfalls (Burns et al., 2002; Fleitmann et al., 2003; Fleitmann et al., 2007). During the humid periods of the Pleistocene and the Holocene, rainfalls reactivated hydrosystems including *wadi* (*wadi*: local name for river and valley) (Hoffmann et al., 2015; Breeze et al., 2016), interior lakes/wetlands (Rosenberg et al., 2012), interdunal lakes (Radies et al., 2005) and extended mangrove environments (Berger et al., 2013; Lézine et al., 2017). However, studying the timeframe of these periods is challenging due to heterogeneity in both the regional and local onset and duration of humid periods and their impacts on the environment. (Preston et al., 2015; Lézine et al., 2017). This heterogeneity is linked to differences between the paleoclimatic archives themselves, recorded processes, preservation qualities and errors inherent to each archive (Berger et al., 2012; Parton et al., 2015). As a result, the reconstruction of quaternary climatic fluctuations in Oman and their impact on the environment and natural resources required more local-scale study in specific Omani environment (*e.g.,* inner mountains, piedmonts, low-lands, etc.). For now, reference data for quaternary climatic fluctuations in northern Oman are the speleothems from Hota Cave ((Fleitmann et al., 2003; Fleitmann et al., 2007; Fleitmann and Matter, 2009).

1.2. Chronology of the Late Pleistocene and the Holocene humid periods

During the late Pleistocene, three pluvial periods are recorded within Marine Isotopic Stage (MIS) 5, the first one during the MIS 5.e (ca. 135,000-120,000), the second one during the MIS 5.c (ca. 115,000-105,000) and MIS 5.a (ca. 85,000-75,000) (Fleitmann et al., 2003; Fleitmann et al., 2007; Fleitmann and Matter, 2009; Rosenberg et al., 2012; Parton et al., 2015). For the MIS 3/MIS 2 (from 35,000 to 20,000 BP), a pluvial period—or phase—has been identified using continental records (lakes and fluvial archives) from the southern Rub al'Khali and the Yemen (McClure, 1976; McLarens et al., 2008; Parton et al., 2013; Sanlaville, 1992), and recently Parton et al. (2013) have suggested an ealier pluvial period from 60,000 to 50,000 BP. The Last Glacial Maximum is considered to be hyper-arid (Parker, 2009). The Holocene Humid Period roughly lasted from 10,500 to 6,000 BP (Clark et Fontes, 1989; Fleitmann and Matter, 2009; Engel et al., 2012). Speleothems records from Hota cave indicate that rainfall was less important in this period than during the Pleistocene humid periods (Fleitmann et al., 2003; Van Rampelbergh et al., 2013) and reached 400 to 500 mm/year in the northwestern piedmont of the Hajar Mountains (Wahalah, Fujairah, UAE) (Preston et al., 2015). The timing of the end of the Holocene Humid Period is particularly debated. On one hand, the transition towards the current arid conditions in some areas has been punctuated by short pluvial episodes, visible in lacustrine and fluvial archives in Northern Oman (Urban and Buerkert, 2009), UAE (Parker et al., 2006) and Yemen (Berger et al., 2012), especially at the beginning of the Early Bronze Age, around 5,200 BP (Parker et al., 2006). On the other hand, short arid episodes have been registered at 8,200 BP, 5,000 BP and 4,200 BP (Fleitmann et al., 2007; Preston and Parker, 2013) along with more stable arid periods, for example between 5,900 BP and 5,300 BP (Preston et al., 2015). Finally, studies based on lagoonal deposits from North and Eastern Oman by Lézine et al. (2017) and calcareous tufa from Dhofar by Cremaschi et al. (2015) suggested that the end of the Holocene Humid Period was characterized by the progressive weakening of the Indian Monsoon due to the southward migration of the ITZC rather than its sudden interruption, which can explain the spatial differences in the termination of the Holocene Humid Period. Arid conditions are observed in all Omani terrestrial records between 4,200 BP and 3,500 BP (Jorgensen and al-Tikriti, 2002; Parker et al., 2006; Cremaschi et al., 2015; Preston et al., 2015).

Northern Oman is currently dominated by arid conditions, with rainfall ranging from 250 mm/year in the Hajar Mountains to less than 50 mm/year in the Rub al'Khali desert. For the southern piedmont of the Hajar Mountains, an area both outside the influence of orographic rainfall and near to the lowlands of the Rub al'Khali basin, there is no data available on Late Pleistocene-Holocene climatic fluctuations and its local impacts on hydrosystems.

1.3. Fluvial archives as records of hydro-climatic fluctuations in Northern Oman

Blechschmidt et al. (2009) demonstrated that the Pleistocene alluvial fans of the southern piedmont of the Hajar Mountains, are correlated with climatic forcing because aggradation phases were recorded during humid periods (mainly during MIS 11, MIS 9 and MIS 7) and happened synchronously with speleothems growth (Blechschmidt et al., 2009; Fleitmann et al., 2007). In this region, fluvial archives offer the possibility to capture a wider range of changes in hydroclimate dynamics than speleothem records that required ~350 mm of annual precipitation to start growing (Fleitmann et al., 2011). For instance, in the western piedmont of the Hajar Mountains, Mueller et al. (2022) identified periods of fluvial activity during the MIS 4 and MIS 2, which are defined as arid periods. Fluvial aggradation phases linked to the Holocene Humid Period thus far have been documented in Northern Oman in only two studies (Fuchs and Buerkert 2008; Urban and Buerkert, 2009). Nevertheless, the rhythms and factors that led to the formation of alluvial terraces remain poorly known, the timescale of the morphological adjustment of wadi-beds has been badly estimated and the (probably) asynchronous upstream-downstream reactions of hydrosystems to a change in water flow and sediment discharge are rarely connected with inherited alluvial landforms at a watershed-scale.

1.4. Fluvial records and geoarchaeological implications

Increased moisture within hydrosystems during pluvial periods allowed for the development of denser vegetation cover and favored the circulation/occupation of animals and humans in areas that are nowadays barren. These periods of "green Arabia" have been recently more deeply investigated due to the key role they seem to have played in the circulation and settlement of the first people in Arabia (Petraglia et al., 2015; Petraglia et al., 2020). During the Pleistocene, major hydrosystems act as a humid axis or "green corridor" for hominin dispersal, including for movements of Homo sapiens out of Africa (Breeze et al., 2016). In contrast, hunter-gatherers were likely living in refugia along the coastline during arid periods (Rose et al., 2018). During the Early Bronze Age (~5,200 to 4,000 BP), archaeological site distribution is clearly organized along wadis and settlement or buildings such as the so-called "towers" can be even located on overbank areas (Beuzen-Waller et al., 2018; Desruelles et al., 2016; Kondo et al., 2014). During the Early Bronze Age, a portion of populations living in the Hajar Mountains, and its piedmonts developed a sedentary lifestyle associated with agricultural practices (Mery, 2013), however evidence of irrigation and agricultural practices remains limited and scattered (Charbonnier, 2014). From the Early Iron Age (3,250 to 2,250 cal. BP), there is clearer evidence for long-term settlements and agriculture in Central Oman (Yule, 2014), along with irrigation practices (Purdue et al., 2019) supported by the discovery of the falaj technology (Cremaschi et al., 2018). The timing and impact of the aridification at the end of Holocene Humid Period on surface flow are key components in understanding the local environmental settings and potentialities surrounding archaeological sites and the history of water resources availability and management during protohistoric periods.

With this study, we aim to provide new data on fluvial records from northern Oman and contribute to the ongoing discussion on climate forcings and early population of Oman. We select as a study site the Wadi Dishshah, a small-scale hydrosystem, that offers appropriate archives to record local hydro-climatic evolution in the lower piedmont of the Hajar Mountains, thanks to its potential to be highly reactive to rainfall events.

2. Geographical and Archaeological Context

2.1. Geographical setting of the Wadi Dishshah

The Hajar Mountains (or Oman Mountains) are located in the northern part of the Sultanate of Oman (fig.1A). The mountain chain is about 650 km long, 40 to 120 km wide, and reaches and elevation of 3,000 m in the Jebel Shams. The Salakh Arch is an anticlinal chain and the last mountainous fold before hundreds of kilometers of desert gravel and the Rub al'Khali basin in the lower

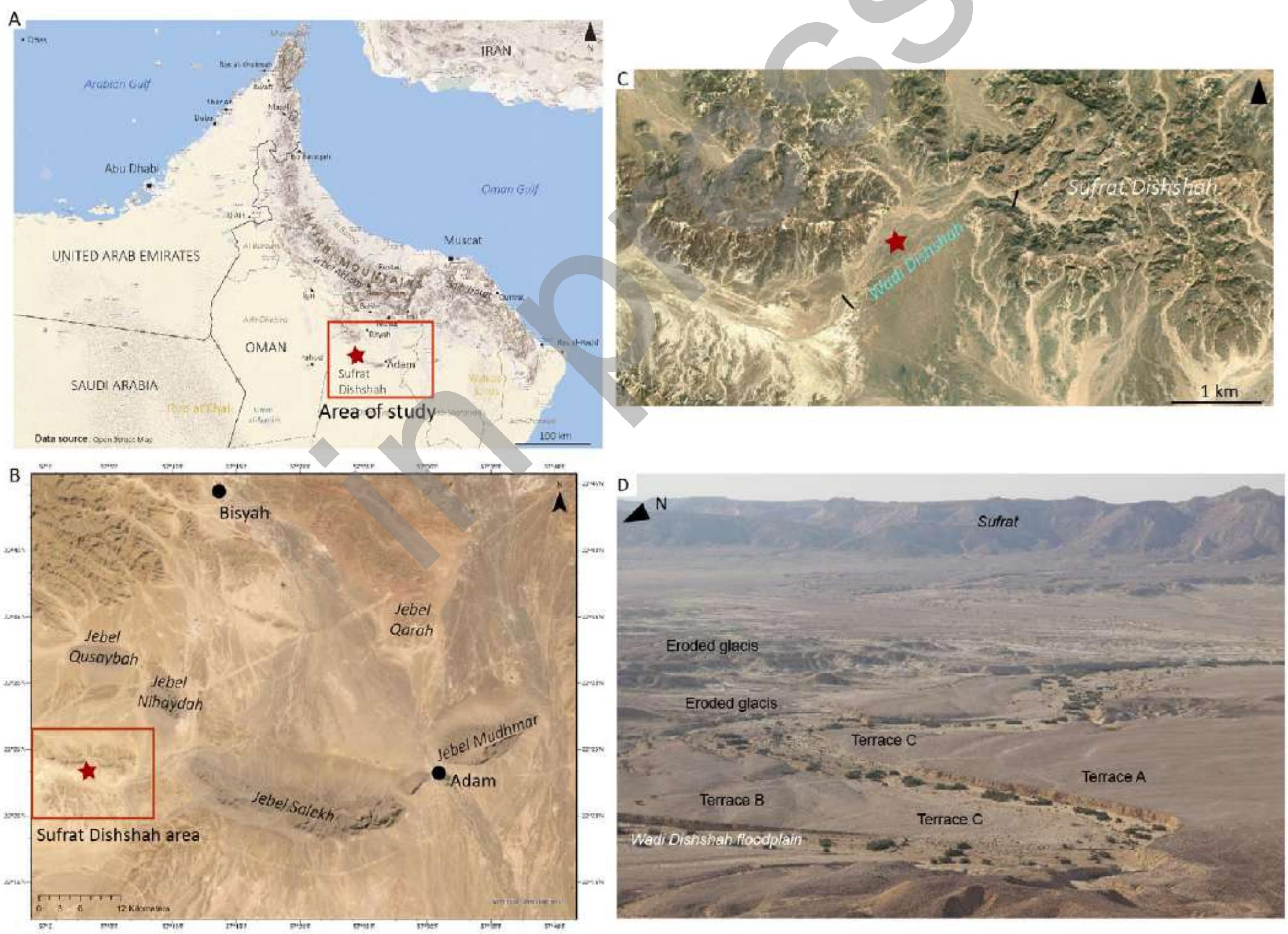

Fig. 1 – Location of the Area of Study and the Wadi Dishshah.

A: Location of the area of study in Northern Oman B: The Salakh Arch chain and Sufrat Dishshah position; C: satellite image (source: Google Earth) of the Wadi Dishshah and section of study; D: Annotated picture of the studied section in Wadi Dishshah (see the geomorphological map for the landforms).

Fig. 1 – Localisation de la zone d'étude et du Wadi Dishshah.

A : Position de la zone d'étude dans le nord du Sultanat d'Oman ; B : La chaine de l'arche de Salakh et la localisation du Sufrat Dishshah ; C : Image satellite (source : Google Earth) du Wadi Dishshah et position du tronçon étudié ; D : Photographie commentée de la section étudiée dans le Wadi Dishshah (voir la carte géomorphologique pour les formations).

part of the southern piedmont of the Hajar Mountains area. It is considered to be the southern-most range of the Hajar Mountains. The Wadi Dishshah is a small watercourse taking its source in one of the mesas ("sufrat" in Arabic) (fig.1B) surrounding the western side of Salakh Arch. The sufrats are made of Late Cretaceous marl (Fiqa Formation Kfq and Kfql), and structured with calcarenite and chert veins (Béchennec et al., 1992; Searle, 2019). The surface of the Sufrat Dishshah is around 400 m above sea level.

The Wadi Dishshah watershed (40 km^2) can provide a high volume of sediments because of its very erodible lithology and the practically non-existent vegetation covering its steep slopes. We assume that its watershed might be reactive to rainfall events despite no evidence of flow being observed during fieldwork between 2013 and 2018. The studied section (fig.1C-D) is 2.2 km long and 5.5 km^2 wide, located within the transition zone of the watercourse between the steep slopes of the mesa and the low-land which consist on a marly ablation glacis incised by wadi stream. The Wadi Dishshah floodplain is currently dominated by vertical erosion, downcutting the marly bedrock via incision. Most of the pebbles are sub-rounded and coming from the chert veins crossing the Wadi Dishshah catchment, gravels furniture is coming from the calcarenite. In nearby Adam, the current climate is arid with mean annual precipitations of around 70 mm/year (climatic data provided by the data portal of the "National Center for Statistics and Information" - Sultanate of Oman (data from 2004 to 2018)). This area, less affected by orographic rainfall rather than the central part of the Hajar Mountains, can be considered as representative of the lower piedmont environmental conditions more broadly.

2.2. Archaeological data for the Salakh Arch and the Wadi Dishshah

More than 3000 archaeological sites have been discovered in the Salakh Arch area by the French Archaeological Mission in Central Oman project between 2007 and 2013 (Giraud et al., 2012; Gernez and Giraud, 2015; Giraud and Gernez, 2016). Archaeological sites range in date from the Paleolithic to the Islamic periods. Paleolithic sites (≥ 300,000 BP to ~8,000 BP) have been found exclusively in the Sufrat Dishshah area (Bonilauri et al., 2014; Beshkani et al., 2017) whereas Neolithic sites (from ~ 8,000 to 5,150 BP) have been found around the Salakh Arch (Lemée et al., 2013).

During the Bronze Age, the spatial distribution of archaeological sites greatly evolves from the Early Bronze Age to the Middle Bronze Age (~5,150 to 3,550 B.P. / 3,200 to 1,600 B.C.) (Gernez and Giraud, 2015; Giraud and Gernez, 2016) indicating a potential reorganization of the occupation around areas where water resources were more easily reachable (Beuzen-Waller et al., 2018). Archaeological sites from the Early Iron Age (~3,250 to 2,250 B.P. / 1,300 to 300 B.C.) are better spread over the Salakh Arch area, over several locations (Beuzen-Waller et al., 2018). This 'continuity' in the occupation/reoccupation of the Salakh Arch area is particularly interesting and allows for a long-term observation of settlement strategies, which seem to be clearly guided by the availability and the reachability of water resources.

3. Material and methods

3.1. Aerial survey and topographic data

The Wadi Dishshah area has never been surveyed before, therefore the only available geographic data was provided by Google Earth satellite imagery and ASTER GDEM (Advanced Spaceborne Thermal Emission and Reflection Radiometer Global Digital Elevation Model) altimetry data. The ASTER GDEM data was not accurate enough to highlight the low topographical variations (fig. 2A) and does not help with the identification of distinct alluvial terrace levels. To overcome this, aerial topographic surveys were conducted using eBee models drone (fig. 2C). Four flights of 45 min were made to cover an area of 5.81 km^2. 1,637 pictures have been processed using the PostFlight Terra 3D software. Processing consisted of three phases. First, an aerotriangulation phase, followed by a densification phase (and finally the production of a Digital Elevation Model (fig. 2B) and an image (orthophotography) in the GeoTIFF format (fig. 2D). The mean 3D resolution of the obtained DEM is 3.14 cm. Georeferencing is based on geotags from source pictures (UTM WGS 84 40 N), with an accuracy of 50 cm to 1 m for XY data and 1.5 m for Z data. The DEM and the orthophotography are used to identify and delineate several topographic levels related to alluvial terraces or a palaeochannel imprint. The DEM was also used to produce topographic profiles with ArcGIS (surface analysis tool).

3.2. Geomorphological mapping

Fieldwork operations complemented the data obtained using the DEM and the orthophotography and enabled us to precisely map the alluvial formations along the Wadi Dishshah. Fieldwork was spread out over three 10-day operations between 2014 and 2016. Mapping was first undertaken within the frame of a GIS (ArcGIS software) and the final layout produced *via* image software (Adobe©). This map focuses on alluvial sheets, cut into three terrace levels, called TA, TB and TC (ranked by size and age) and on ablation glacis units: G is used to denominate the main glacis and GE to indicate several flat glacis units (fig. 3).

3.3. Section studies: morphostratigraphy and malacological Analyses

The map of the Wadi Dishshah alluvial formations leads to the identification of several representative sections (TA-1; TB-1; TB-2; TB-3; TC-1) (fig. 3-4). Each section was first cleaned and rectified. Individual sedimentary unit were recorded and documented with a SU number; the sedimentary texture was described during the fieldwork. Fluvial deposits' architectural information was summarized in detailed sketches. The malacological remains studied comes from the TB-1 section, which was the only section to present many mollusks, where 6 litres of sediment were sampled from each SU. The sediment was sieved through a 2 mm mesh, allowing for the retrieval of many shells. The species have been identified according to the literature (Neubert, 1998), with a distinction between adults and

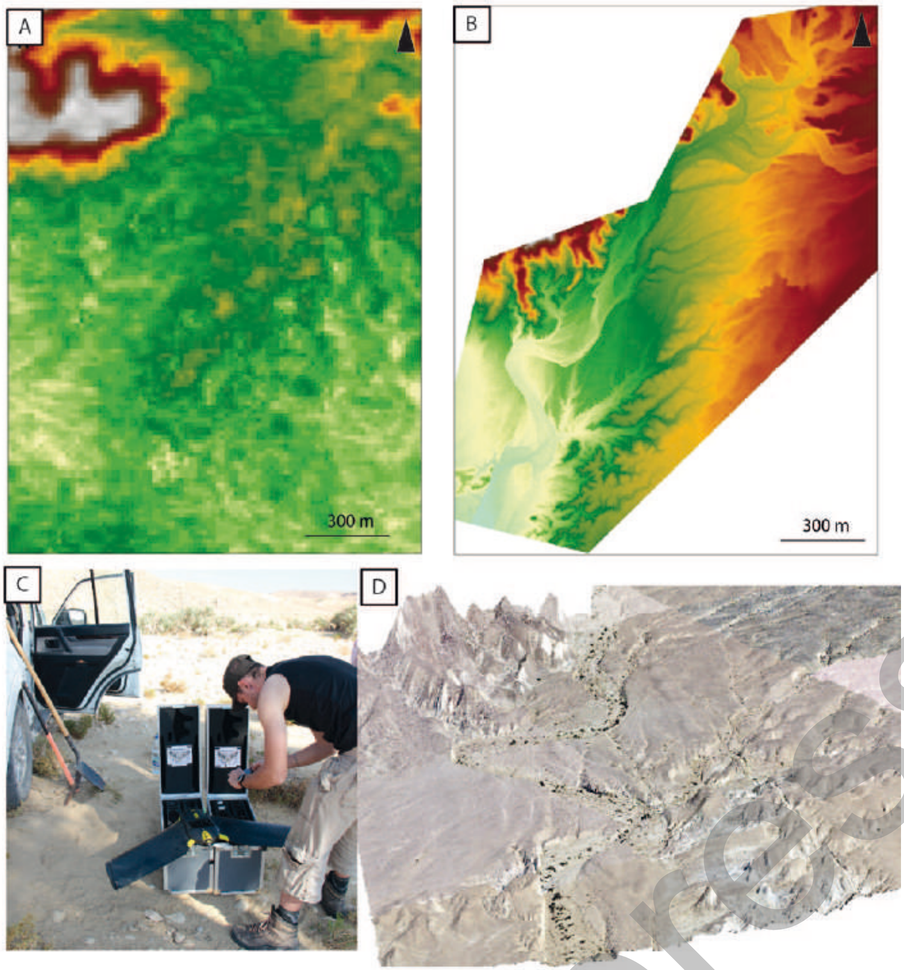

Fig. 2 – Available DEM and Aerial Survey Realized in the Wadi Dishshah.

A: ASTER GDEM raster data available for the Sufrat Dishshah; B: DEM obtained with the aerial survey; C: Julien Guery from Captair company preparing eBee drone before a flight; D: Orthophoto of the Wadi Dishshah covering the DEM data.

Fig. 2 – Modèle Numérique d'Elevation (MNE) disponible et prospection aérienne réalisée dans le Wadi Dishshah.

A : Données ASTER GDEM disponibles pour le secteur du Sufrat Dishshah ; B : MNE obtenu à l'issue de la prospection aérienne ; C : Julien Guery de la compagnie Captair préparant un drone Ebee avant un vol ; D : Orthophotographie du Wadi Dishshah drapée sur le MNE.

juveniles. The malacological study is qualitative because we have less than 300 individuals per unit.

3.4. Chronology: OSL, radiocarbon and relative age-dating

Absolute chronology relies on both OSL (Optically Stimulated Luminescence) and radiocarbon dating. OSL samples were studied in the Geoluminescence Dating Research Laboratory (Baylor University, Waco, Texas) (tab. 1). Quartz fractions were analyzed under blue-light excitation (470 ± 20 nm) with single aliquot regeneration protocols (Murray and Wintle, 2003). The central age model of Galbraith et al. (1999) was used to calculate the equivalent dose with overdispersion values ≤ 20% (one sigma error); the sample with the highest overdispersion values was analyzed using a "Finite Mixture Model" (Galbraith and Green, 1990). Two samples of charcoal remain from the section TB-3 were hand-collected and were sent to the Beta Analytics laboratory for radiocarbon dating (tab. 1). Conventional ages were recalibrated by the authors using the Calib 7.0 softwareÓ (Stuiver and Reimer, 1993) and the "IntCal20 Calibration Curve" (Reimer et al., 2020) and presented with a 2-sigma error. Median and calibrated age for OSL age-dating was calculated with ChronoModelÓ version 2.0 (Lanos and Dufresne, 2019) (tab. 1). In the text, age-dating are presented with median cal. BP results that have been rounded to the nearest hundred, intervals and conventional ages are visible in Table 1. Relative age-dating using surface archaeological artefacts has been used with the glacis formation.

4. Results

4.1. Malacological study

In the assemblage of malacological remains, 1,133 specimens were identified (631 adults and 502 juveniles) (fig. 6). Because the Arabian Peninsula is one of the driest areas in the world, only few species of snails can survive without water with an aerial breathing system during a short period (Neubert, 1998). Therefore, the assemblage was composed of only two species: *Zootecus insularis* (Ehrenberg, 1831), and *Pupoides coenopictus* (Hutton, 1834). Both belong to the holo-Saharo-Sindian group. They are often found together within assemblages (Amr and Al-Shammari, 2013; Neubert, 1998; Pietsch et al., 2010; Pietsch & Kühn, 2012; Purdue et al., 2021). The snail *Z. insularis* is quite ubiquitous, robust and survives short drought periods thanks to aerial breathing. *Z. insularis* can be found in moister environments within shaded (Al-Khayat, 2010) or mangrove contexts (Khanam et al., 2020), while *P.coenopictus* can occur in riverbank or lacustrine contexts (Matter et al., 2015; Radies

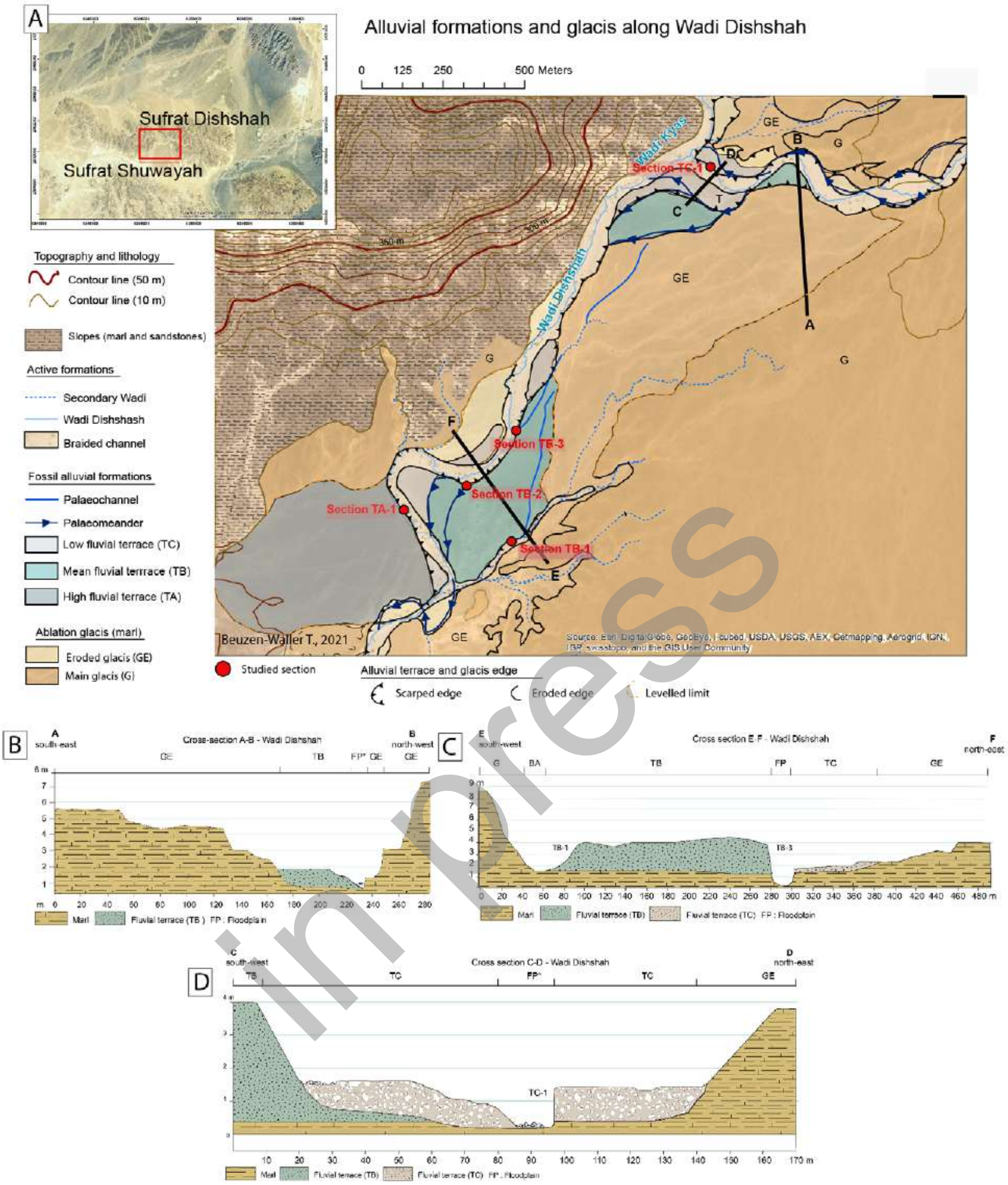

Fig. 3 – Geomorphological map, cross-sections, and position of the studied section.

A: Geomorphological map of the Wadi Dishshah focused on alluvial formations and glacis, location of studied sections and transect; B: Transect A-B; C: Transect C-D; D: Transect E-D.

Fig. 3 – Carte géomorphologique, transects et localisation des coupes étudiées.

A : Carte géomorphologique centrée sur les formations alluviales et les glacis, transect et position des coupes étudiées ; B : Transect A-B ; C : Transect C-D ; D : Transect E-D.

et al., 2005). In TB-1, juveniles of both species have been identified (*P. coenopictus*: 809 NISP, 505 adults, 304 juveniles; *Z. insularis*: 324 NISP, 126 adults, 198 juveniles), meaning that the environment was suitable for the reproduction of mature specimens, egg-laying and the birth of juveniles. *Z. insularis* are most abundant at the base of the section and decreased quickly, while *P. coenopictus* increased in abundance from SU 4 with its highest representation in SU 10 and SU 11. For both species, high occurrences occurred in UF 4 and 10. At the end of the occupation, both species declined in abundance.

Tab. 1 – Age-dating obtained in this study.

Tab. 1 : Datations obtenues dans cette étude.

Samples name	Lab number	Aliquots[1]	Grain size (µm)	Equivalent dose (Gray)[2]	Over dispersion (%)[3]	U (ppm)[4]	Th (ppm)[4]	K (%)[4]	H20 (%)	Cosmic dose (m Gray/yr)[5]	Dose rate (m Gray/yr)	OSL age (yr)[6]	HPD 95% age cal. BP[7]	Median cal. BP[7]	HDP 95% cal. BC[7]	Median cal. BC/AD[7]
TA-1-a	BG 4210	33/35	100-63	20.55 ±0.96	18±2	1.32 ±0.01	1.24 ±0.01	0.20 ±0.01	3±1	0.17 ±0.02	1.29 ±0.05	26.550 ±1780	23.001-29.973	29.487	-28.023 ; -21.051	-24.537
TA-1-b	BG 4112	23/25	100-63	6.89 ±0.68	74±10	1.14 ±0.01	0.61 ±0.01	0.10 ±0.01	3±1	0.19 ±0.02	0.30 ±0.03	11.390 ±1270	8.838-13.816	11.327	-11.866 ; -6.888	-9.377
TB-3-a	BG 4410	57/70	250-355	6.89 ±0.68	42±4	1.07 ±0.01	0.76 ±0.01	0.23 ±0.01	3±1	0.20 ±0.02	0.70 ±0.03	6.605 ±665	5.236-7.842	6.539	-5.892 ; -3.286	-4.589
TB-1-a	BG 4021	35/39	150-100	8.34 ±0.44	14±2	1.40 ±0.01	3.75 ±0.01	0.66 ±0.01	3±1	0.16 ±0.02	1.34 ±0.07	6.225 ±465	5.248-7.072	6.160	-5.122 ; -3.298	-4.210
TB-1-b	BG 4020	21/33	150-100	6.57 ±0.32	17±3	1.20 ±0.01	2.12 ±0.01	0.48 ±0.01	3±1	0.19 ±0.02	1.07 ±0.05	5.875 ±415	4.996-6.624	5.810	-4.674 ; -3.046	-3.860
TB-2-a	BG 4024	280/35	150-100	8.65 ±0.49	23±3	1.59 ±0.01	3.93 ±0.01	0.79 ±0.01	3±1	0.16 ±0.02	1.56 ±0.08	5.560 ±420	4.672-6.318	5.495	-4.368 ; -2.722	-3545
TC-1-a	BG 4022	23/43	100-63	2.78 ±0.17	24±4	1.45 ±0.01	1.98 ±0.01	0.39 ±0.01	3±1	0.18 ±0.02	1.06 ±0.05	2.620 ±210	1.950-3.605	2.768	-1.655 ; 0	-728

4.2. Geomorphological landforms along the Wadi Dishshah

4.2.1. Organization of the geomorphological units

Two states of glacis (G = uneroded glacis and GE = eroded glacis) and three fluvial terraces (TA, TB and TC) were identified (fig. 3A). In the upstream part of the studied section, the G unit dominates. G is a marlish glacis ~8 m above wadi-bed level, with various flat stairs (GE), shaped when the floodplain was cut down (fig. 3B). GE units are covered with a thin pavement of heterometric gravel. Alluvial accumulations are more visible in the middle and the downstream parts of the studied area, they are organized into three generations of alluvial sheets, incised within three fluvial terrace levels. The highest fluvial terrace (TA) is mainly visible in the downstream part of the section. It has been studied with the TA-1 section, which is located four meters above wadi-bed level. This alluvial accumulation (3 meters thick) covers marl bedrock that has been down cut one meter deep. TB is the intermediate fluvial terrace; the average height of sections (TB-1; TB-2 and TB-3) is around 2.5 m above wadi-bed level. This unit, well developed in the central part of the studied area, also covers the marl bedrock along C-D and E-F transect analysis (fig. 3C-D). The last fluvial terrace is the lowest one (TC), standing 1.5 m above wadi-bed level. It is well developed at the confluence located in the upstream part of the section (fig. 3D). The TC unit is also built on marl or is locally embedded into TB (fig. 3C-D).

4.2.2. Morphostratigraphy

The alluvial accumulation of the TA level visible on the TA-1 section (fig. 4A) is 2.5 m thick. The stratigraphic organization of the unit reveals an aggradation depositional system dominated by braided channels and carrying high-caliber sedimentary loads (pebbles, gravels, coarse sands) at the base of the section and finer sandy/gravel slack water flood sediments at the top of the section. Cross-stratified beds of pebbles/block units (maximum grain-size 15 cm) are visible at the base of the section. These high-discharge units are punctually separated by gypsum crusts. The second stage of the section includes finer sediments. Planar coarse sand units are visible as well as channel fills with gravel.

The alluvial accumulation of the TB level has been studied in three sections: TB-1, a natural section excavated by a gully (fig. 4B); TB-2, a section in the meander (fig. 5B) and TB-3, located on a natural bank presenting a palaeochannel (fig. 5D). The thickness of the alluvial accumulation is around 2.5–3 meters. The base of TB-1 (SU 1-SU 3) is characterized by poorly rounded, tight and heterometric debris or pebbles (max caliber 10 cm), organized in oblique planar beds. From SU 3 to SU 18, horizontal fine laminations, ranging from sand to silt, are visible. SU 4 and SU 15 are darker units (fig. 4B-C) presenting numerous snails and bioturbation and might refer to an ancient soil.

The TB-2 section is included in a large lateral accretion macroform (fig. 5A) related to the depositional lobe of the meander. Several cross-bedding stratifications are bending to the north. Facies visible in TB-2 are heterogeneous (fig. 5B). At the base, it includes gravel beds covered by medium-to-coarse sand units (from SU 1 to SU 8). Finer, greyish settling deposits (SU 10) are covered by evaporites (gypsum crust). Carbonate concretions are visible in SU 12. The end of the section is covered by aeolian sand deposits (cross-stratified sorted fine-medium sands).

The base of TB-3 (from SU 1 to SU 11) presents similar facies to the base of TB-1 and is also built directly on marl. This suggests an extended high-energy sheet at the base of all the TB terrace level. Still in TB-3, laminated coarse units (from classified gravel to coarse sand) suggest several flooding episodes (from SU 2 to SU 11). One palaeochannel is visible in the TB-3 section between SU 12 and SU 44. The sedimentary structures are mostly laminar but do not extend much and are organized in many small units, alternating between coarse and silty sands.

The alluvial accumulation of the TC level (fig. 5C) is mainly composed of heterometric blocks (up to 15 cm caliber) and clast-supported gravel deposits. Sediments are unsorted, and sandy units are very scarce.

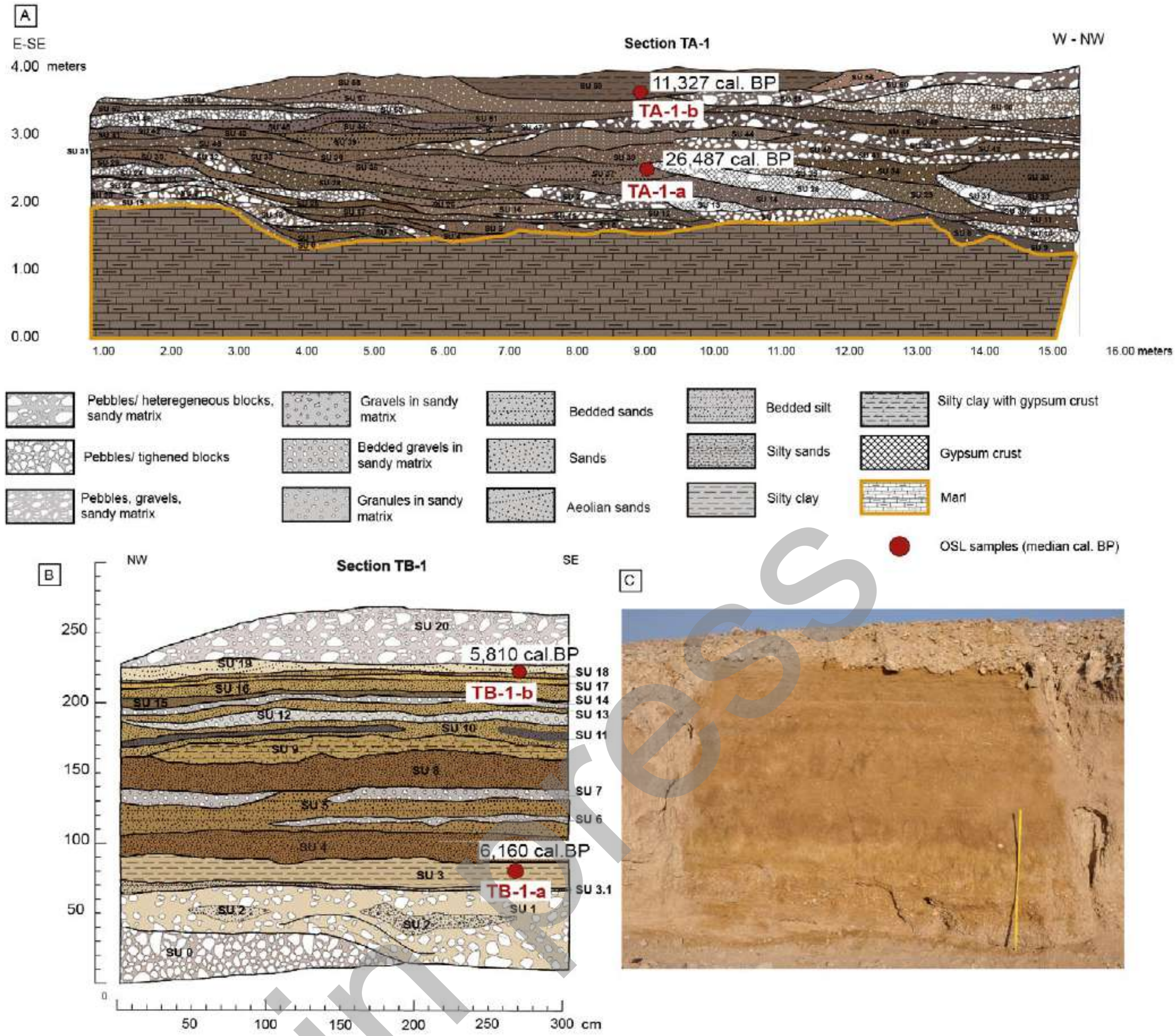

Fig. 4 – Sketches and pictures of sections TA-1 and TB-1.

A: Section of the section TA-1 and position of the samples; B Section TB-1 and position of the samples; C: Picture of TB-1. Legend is common for both sections.

Fig. 4 – Schéma et photos des coupes TA-1 et TB-1.

A : Schéma de la coupe TA-1 et position des échantillons ; B : schéma de la coupe TB-1 et position des échantillons ; C : photo de TB-1.

4.3. Chronology

The erosion of GE has been dated relatively using Palaeolithic artefacts found on the surface of the Sufrat Dishshah glacis during previous archaeological surveys (Bonilauri et al., 2014). The density of artefacts is smaller on the eroded part of the glacis (GE), which might indicate that the surface has been scraped by floods. The typo-technological traits of the artefacts found on G are related to Middle and Upper-Late Palaeolithic assemblages (Bonilauri et al., 2014), the *terminus ante quem* provided by the artefacts can extend until as recently as 7,000 BP (Rose et al., 2018).

The bottom of TA-1 dates to 26,550 ± 1,270 years (26,487 cal BP: median cal. BP age calculated with ChronoModel, rounded age 26,500 cal. BP, intervals are visible in Table 1). The top dates to 11,390 ± 1,270 years (11,387 cal. BP, rounded age 11,300 cal. BP) (tab. 1, fig. 4A). The base of TB-1 (SU 3) is dated to 6,225 ± 465 years (6,610 cal. BP, rounded age 6,200 BP) and the upper part of the section (SU 18) to 5,875 ± 415 years (5,810 cal. BP, rounded age 5,800 cal. BP) (tab. 1, fig. 4B). SU 9 of the TB-2 section has been dated by OSL to 5,560 ± 420 years (5,495 cal. BP, rounded age 5,500 cal. BP). In TB3, the base of the section dates to around 6,605 ± 665 years (6,539 cal. BP, rounded age 6,500 cal. BP). In the paleochannel, the finding of charcoal allows for dating SU 20 via radiocarbon: 5,040 ± 30 BP (5,821cal. BP, rounded age 5,800) and SU 37 at the top of the section: 4,970 ± 30 BP (5,684 cal. BP, rounded age 5,700 cal. BP) (tab. 1, fig. 5D). Finally, only one age-dating (OSL) is available for TC: 2,620 ± 210 years (2,768 cal. BP, rounded age 2,800 cal. BP) (tab. 1, fig. 5C).

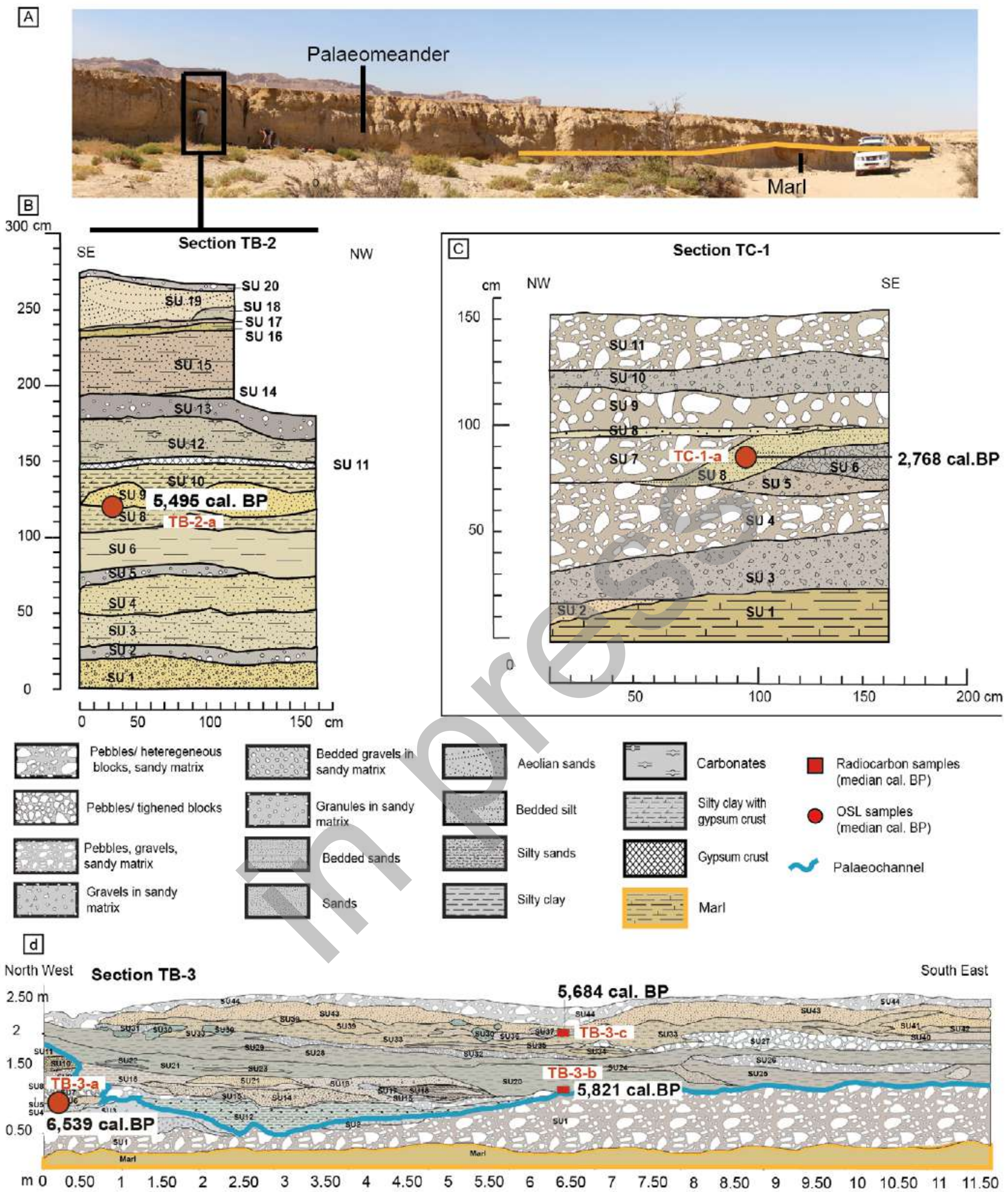

Fig. 5 – Sketches and pictures of sections TB-2, TB-3 and TC-1.

A: Panoramic picture (towards south) of the meander and position of theTB-2-section; B: Sketch of the TB-2 section and sample location; C: Sketch of the TC-1 section and sample location; D: Sketch of the TB-3 section and samples location. Legend is common for both sections.

Fig. 5 – Schéma et photos des coupes TB-2, TB-3 et TC-1.

A : Photo panoramique (vers le sud) du méandre et position de la coupe TB-2 ; B : Schéma de la colonne étudiée TB-2 et position des échantillons ; C : Schéma de la colonne étudiée TC-1 et position des échantillons ; D : Schéma de la coupe TB-3 et position des échantillons.

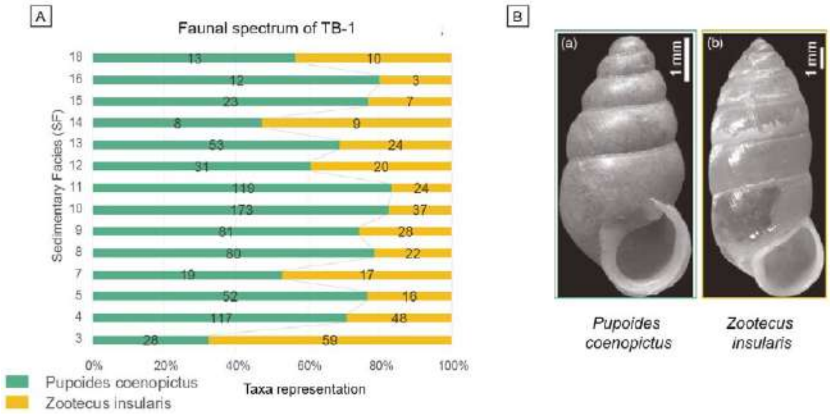

Fig. 6 – Malacological assemblage of TB-1.

A: Faunal spectrum of TB-1, distribution of snails per taxa and sedimentary facies (both adult and juveniles' specimen); B: Pictures of the two identified species (*Pupoides coenopictus* and *Zootecus insularis*).

Fig. 6 – Assemblage malacologique de TB-1.

A : Spectre faunique de TB-1, répartition des mollusques par espèces et par facies sédimentaires (individus adultes et juvéniles ensemble) ; B : Photos des deux espèces identifiées (Pupoides coenopictus and *Zootecus insularis).*

5. Discussion

5.1. Evolution of the Wadi Dishshah over the last 26,000 years and regional comparison

The study of the Wadi Dishshah section suggests that three phases of aggradation and three phases of incision have taken place since 26,000 BP and led to the development of fluvial terraces (fig. 7).

5.1.1. Incision of G and base of TA's aggradation around 26,500 cal. BP

The incision of G in several levels (GE) happened progressively during the downcutting phase of the Wadi Dishshah. The data is not sufficient to conclusively connect the incision process to climatic or tectonic forcing. Artifacts found on the GE surface suggest that it became stable around 7,000 BP (fig. 7A).

TA's aggradation started around 26,500 cal. BP during the MIS 2, which is considered to be an arid period (Parker, 2009; Parton et al., 2015). Salt crust visible at the base of section TA-1 may indicate extended drought periods. Considering the geometry and orientation of the pebbles/gravel sheets, this deposit is interpreted as a gravel-bed braiding river with several gravel bars due to high-energy streams fueled by intense rainfall. Lateral inputs of sediments coming from the rocky slopes might have increased the solid load. Mueller et al. (2022) also identified fluvial activity during the MIS 2, between 20,000 – 17,000 BP, but characterized by low energy channel flow rather than high energy deposits.

The top layer of TA-1 is dated around 11,300 cal. BP at +3.60 m from wadi-bed level (fig. 7B). This date fits with the beginning of the Holocene Humid Period. The thinner bed-load sheets are probably related to less turbulent flow.

5.1.2. Incision and downstream evacuation of alluvium between 11,300 and 6,500 cal. BP

The incision of the TA alluvial sheet happened between 11,300 cal. BP (top of TA-1) and 6,500 cal. BP (base of TB-3), during the Holocene Humid Period (fig. 7C). The Holocene deposits at the top of TA-1 indicate that cutting started at the transition between arid and humid conditions. In this section of Wadi Dishshah, downcutting of the valley might have coincided with flows reactivation during the Holocene Humid Period and the capacity of rivers to remobilise solid loads previously deposited by a decelerating and overloaded wadi. The chronological hiatus between the top of TA and TB falls precisely during the maxima of the Holocene Humid Period identified in speleothems (Fleitmann et al., 2007), tufas (Clark and Fontes, 1989), lacustrine deposits (Parker et al., 2006; Preston et al., 2015) and pollen (Lézine, 2009; Lézine et al., 2017) (fig. 8). It is therefore highly probable that during the Holocene Humid Period's fluvial maxima, the Wadi Dishshah watershed was wider, with the erosion/transfer zone covering the studied area and the depositional zone located downstream. This hypothesis would explain the absence of alluvial aggradation resulting from the Mid-Holocene Humid Period in this section of the Wadi Dishshah and the erosion of the marl bedrock on which TB has developed.

5.1.3. From 6,500 to 5,800 cal. BP, a migrated floodplain with green distal area

The base of the TB-3 (6,500 cal. BP) and TB-1 (6,200 cal. BP) sections suggests an extended floodplain (fig. 7D), where braided and dynamic channels extended over the area currently covered by TB (fig. 4-5). Starting at 6,200 cal. BP (SU 3 TB-1), TB-1 presents overbanks deposits suggesting that part of the plain started to be disconnected with the braided channels and was only fueled by low-energy overflows. We propose that the minor-bed started to migrate northwards at this period (fig. 7E). The malacological remains (fig. 6) indicate wadi banks with green cover and shaded conditions. Optimal conditions were present by the time SU 11 was deposited (distal floodplain "wetland"? More shadow?), when juveniles of both species were strongly represented. Palaeosols in SU 4 and SU 11 are probably contemporaneous with these periods (fig. 4). At the end of the section, around 5,800 cal. BP, both species declined in abundance, which may imply worsening climatic conditions for them. TB's main phase of aggradation occurred during this period, suggesting a progressive upstream migration of the depositional zone of the wadi at the end of the Holocene Humid Period.

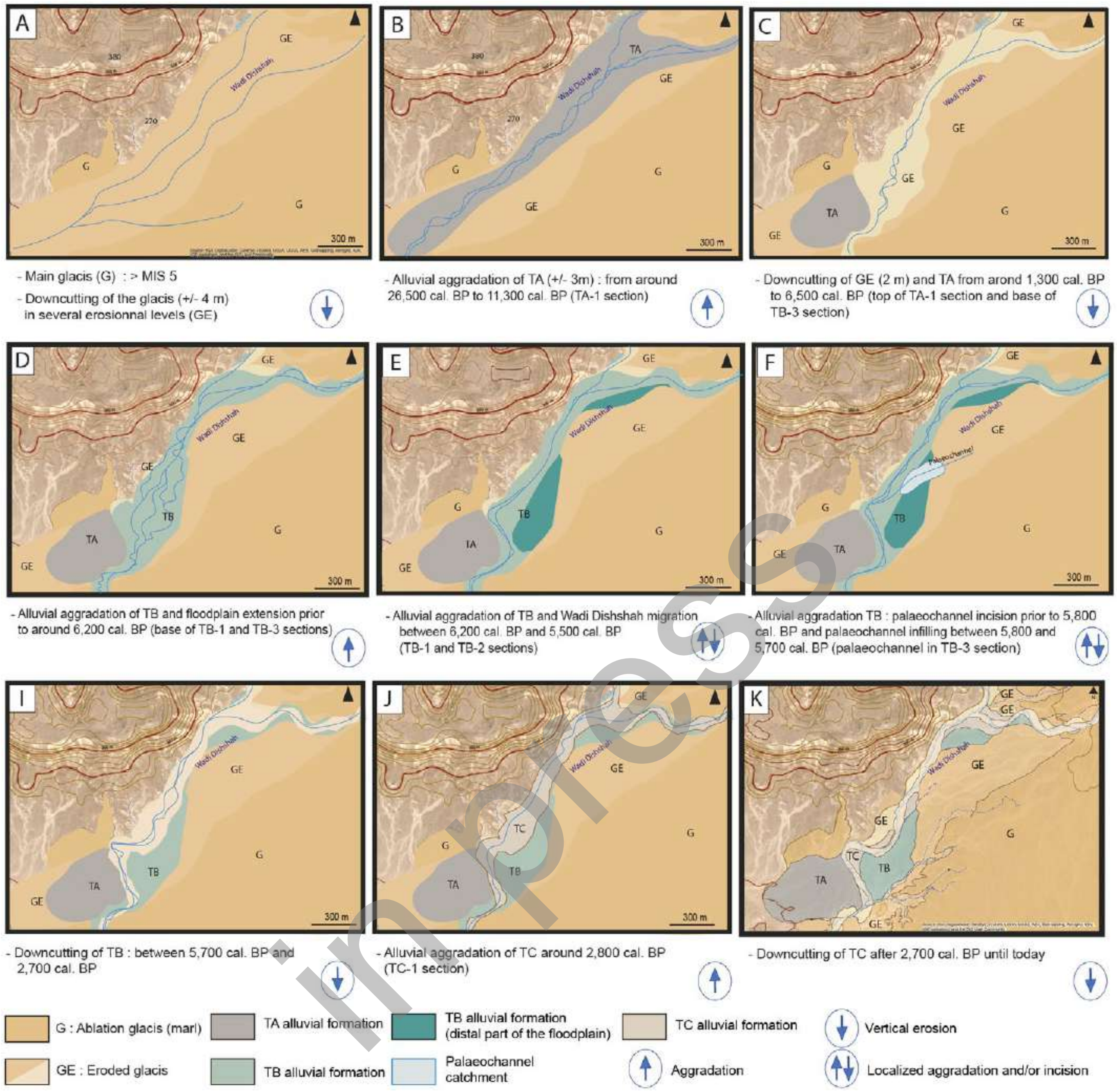

Fig. 7 – Schematic evolution of the Wadi Dishshah since the late Pleistocene (source of the background: Google Earth satellite imagery).

Fig. 7 – Evolution schématique du Wadi Dishshah depuis le Pléistocène supérieur (source du fond de carte : imagerie Google Earth).

5.1.4. From 5,800 to 5,500 cal. BP, incision and infilling of smaller secondary channels

The incision of the alluvial sheet TB by smaller secondary channels (fig. 7F) finding their path to join the floodplain might have happened before 5,800 cal. BP (base of TB-3 palaeochannel in Figure 5), as incision is visible in the palaeochannels in TB-3. The TB-3 palaeochannel was probably filled in between 5,800 cal. BP and 5,700 cal. BP. The infilling is picturing a small, braided channel, littered with several sandy bars and small muddy waterholes. The top of TB is covered by aeolian deposits, which rose to dominance afterwards. The formation of the paleochannel is potentially related to the northward migration and narrowing of the Wadi Dishshah floodplain, a slowdown in flow dynamics probably itself associated with decreasing rainfall. The lateral accretional deposits of a lobe meander's construction in Wadi Dishshah (TB-2) (fig. 3, 5) are dated at around 5,500 cal. BP. The numerous salt crusts visible in TB-2 might suggest long-term exposure during extended drought periods.

The infilling of secondary channels and the accretionary deposits associated with channel shifting are the last records for the Holocene Humid Period and the first Holocene hydro-climatic data for the southern part of the Hajar Mountains. This fits with other hydro-climatic data obtained in different parts of the Northwestern Hajar Mountains. Preston et al. (2012) (Awafi lake, UAE) showed that arid conditions started to manifest around 5,900 cal. BP. Organic materials can still be found in lake sediments until 5,500 cal. BP. However, sediments are found to be completely aeolian in origin at around 5,000 cal. BP. In Wahalah lake (UAE), four meters of aeolian deposits clogged the lake sometime between 5,900 and 5,200 cal. BP (Parker et al., 2016). The onset of arid conditions has been traced to around 5,000 cal. BP in the northern lagoon (Sur, coastal piedmont of the Hajar Mountains, Oman) by Lézine et al. (2017) (fig. 8). Compared to the coastal piedmont, we can clearly see an earlier onset of arid conditions in these southern arid margins of the Hajar Mountains.

5.1.5. Around 2,800 cal. BP: TC aggradation and a short pluvial phase?

TB's downcutting happened sometime between 5,500 cal. BP and 2,800 cal. BP, likely after arid conditions began to develop (fig. 7I). This is a phase of major vertical erosion, around three meters in depth (fig. 3C-D). TC accumulation happened around 2,800 cal.BP turned out to be a surprising source of information because of the high caliber of the bedload present over 1.50 m of accumulation (fig. 7J). This material hints at intense rainfalls. It is difficult to evaluate whether TC's alluvial deposits are the result of one or several series of strong, short-term precipitation events or a more pronounced pluvial episode because there is only one age estimation available. This detritism cannot be the result of anthropogenic forcing, such as land clearing or wood exploitation, because the Sufrat Dishshah was not occupied during the Bronze Age and the Iron Age. However, fluvial activities characterized by detritism have been identified in other parts of south-eastern Arabia at the same period. In the oasis of Masafi (north-western Hajar Mountains, UAE), flow dynamics have been observed between 3,200 and 1,800 BP, with an important phase of detristism between 2,300 and 1,800 BP (Purdue et al., 2019). At Rustaq (northern piedmont of the Hajar Mountains, Oman), runoff activity linked to agricultural practices during the Early Iron Age has been observed at around 2,300 BP (Purdue et al., 2021). In the Hadramawt Basin (Yemen), Berger et al. (2012) identified a late aggradation in the Wadi Masila fluvial archives between 2,769–2,383 cal. BP and 2,347–2,151 cal. BP (fig. 8). Lezine et al. (2017) found traces of Rhizophora mangrove trees dating back to sometime between 2,500 and 2,000 cal. BP in pollen records from the Rwar al Jaramah lagoon (Oman). Similar remains were found in Filim lagoon (Oman), dating back to sometime between 3,000 and 2,000 cal. BP. The TC aggradation was therefore probably caused by a regional climatic fluctuation, such as a temporary increasing of intense pluvial events, such as storm or cyclone.

5.2. Inputs for fluvial terrace studies in Northern Oman

This study constitutes the first Holocene fluvial records in an undisturbed environment for the southern area of the Hajar Mountains piedmont. Looking at the cessation of speleothem growth in the inner Hajar Mountains at about 6,300–5,200 BP (Fleitmann et al., 2003), which likely happened when average annual rainfall drops lower than 300–350 mm around Hoti Cave (Fleitmann and Matter, 2009), we observed that the Wadi Dishshah reacts within a similar timeframe, but with a gradual adjustment. This demonstrates the relevance of fluvial records for the acquisition of local hydro-climatic data in Oman. It provides an interesting hydro-climatic picture of the Hajar Mountains' arid margins as well as new data on how hydrosystems react at the end of the Holocene Humid Period. In the Salakh Arch area, regular water flow along with denser vegetation cover might have continued until 5,800 cal. BP. A progressive upstream migration of the depositional zone of the wadi started around the same period until 5,500 cal. BP.

The role of Late Pleistocene/Holocene tectonic uplifting into the downcutting phase of the valley floor and the staircase organization of the fluvial terraces has also been considered, but little data exists for Quaternary upliftings in Northern Oman since the Last Glacial Maximum, apart from Moraetis et al. (2018), who examine the eastern coastal piedmont and suggest an uplifting rate between 4 mm/yr and 1 mm/yr. Based on our available age-dating and the incision depth per generation of alluvial forms in the Wadi Dishshah, we calculated an incision rate of about 0.6 to 1.0 mm/year. The Wadi Dishshah is quite far from Moraetis et al. (2018) study areas and we currently have too few dates and data available from our study to consider this possibility in detail here. But it seems unreasonable to completely exclude the influence of tectonic forcing on the downcutting of the valley floors in the Salakh Arch area.

For now, it is also complicated to evaluate the upstream-downstream variability of erosional/aggradation processes along Wadi Dishshah catchment. Additional fluvial studies in the Wadi Dishshah might provide more information on this poorly understood parameter and to allow us to better appreciate the upstream–downstream reactions of this hydrosystem.

5.3. Inputs for geoarchaeology in the Salakh Arch area

In the Salakh Arch area, the distribution of archaeological sites changes considerably from the prehistoric to the protohistoric periods and seems to be closely linked to the localisation and reachability of water resources (Beuzen-Waller et al., 2018). Artefacts from the Upper and Late Palaeolithic (from ~30,000 to 8,000 BP) have been found exclusively in the Sufrat Dishshah area (Bonilauri et al., 2014). For the Pleistocene, the single date obtained during our study does not allow any conclusions. For the Early/Mid Holocene, we propose that the sufrat area benefited from wetter conditions, but the fluvial archives related to this period are likely located downstream the section studied in this paper. For the Neolithic Period (~8,000 to 5,150 cal. BP), fluvial archives reveal more regular flow and extended floodplain in the Wadi Dishshah. These conditions enable occupations of areas that are today dry and barren, like the Jebel al'Aluya (Lemée et al., 2013). The drying up of the Wadi Dishshah is not exactly synchronous with the reorganization of archaeological sites. Indeed, surface flows are visibly reduced around 5,500 cal. BP in the Wadi Dishshah but the archaeological site distribution indicates a concentration on hydrologically-favoured areas (e.g. gap outlets of the Salakh Arch, see maps in Beuzen-Waller et al., 2018) during the Umm an-Nar period (4,650 to 3,950 cal. BP), and especially the Wadi-Suq Period (3,950 to 3,550 cal. BP). Some hypotheses are suggested here to explain this phenomenon: first, in this part of the piedmont, the

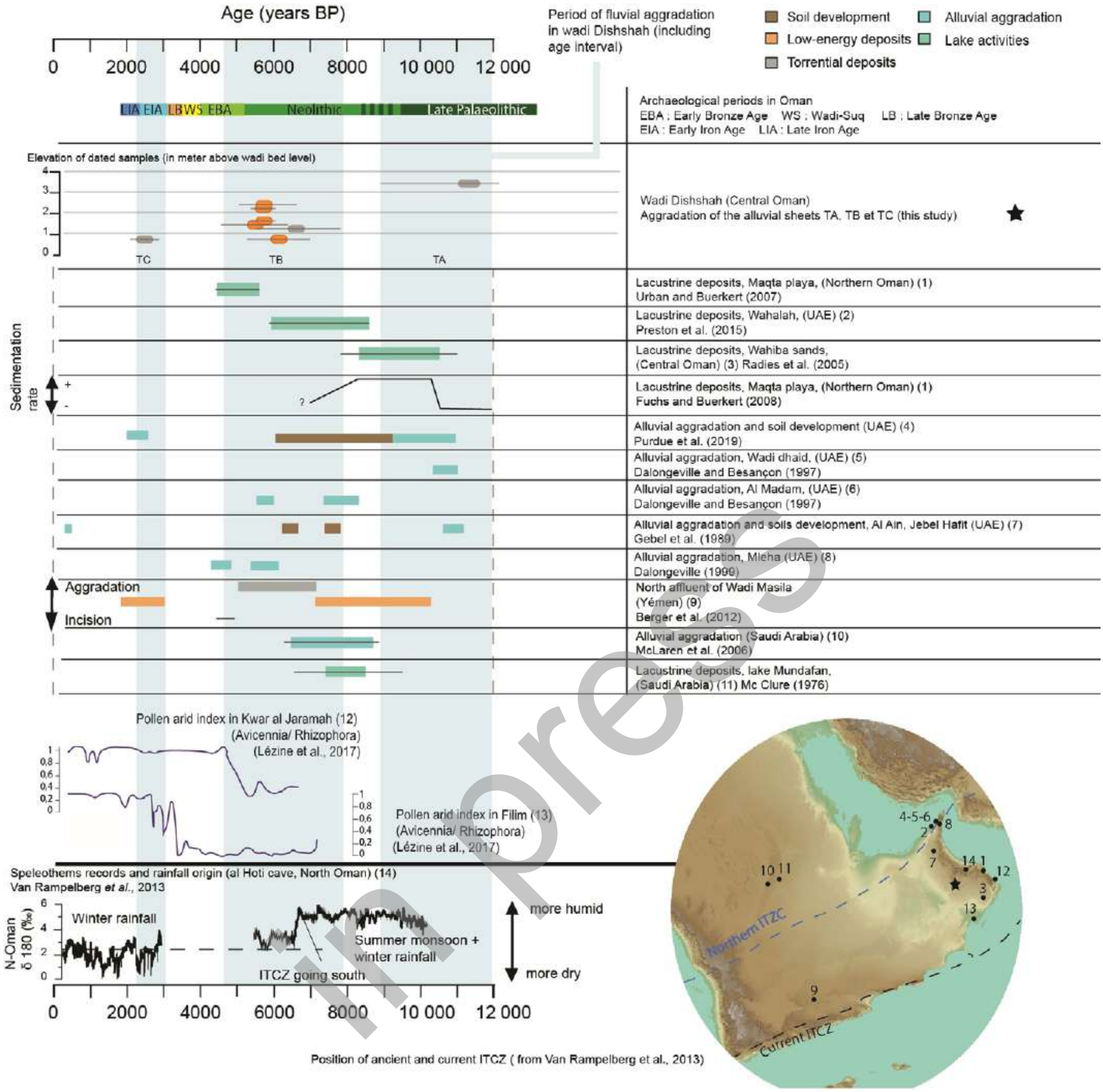

Fig. 8 – Aggradation phases in the Wadi Dishshah and other hydro-climatic data from Oman, United Arab Emirates and Saudi Arabia.

Fig. 8 – Phases d'aggradation dans le Wadi Dishshah et autres données hydro-climatiques obtenues à Oman, aux Emirats arabes unis et en Arabie Saoudite.

strategy for settlement patterns relies more on shallow groundwater than on surface flows; second, the hydrosystems originating in the Hajar Mountains and flowing into the gaps were impacted by aridity later than the Wadi Dishshah; third, the fluvial records provide early information on the impact of aridity on hydrosystems, but the resulting constraints on the environment and the necessary adaptation of impacted human groups only appear after a certain delay. It is also possible that Bronze Age inhabitants of this remote area of the Hajar Mountains piedmont were mobile small-scale societies, as presented by Balbo et al. (2016), characterized by long-term socio-ecological resilience and rapid adaptive responses. Finally, the potential pluvial phase identified in TC at 2,800 cal. BP is synchronous with the spring's activity at the Early Iron Age site of Mudhmar East, dated with tufa deposits to around 2,730–2460 cal. BP (Jean et al., 2021), allowing us to consider more humid conditions during the Early Iron Age, at least in the Salakh Arch area.

6. Conclusion

The study of the fluvial history of the Wadi Dishshah provides the first Holocene alluvial records for the southern Hajar Mountains piedmont. This continental record captured hydro-climatic information for a proximal part of the piedmont, located in a small watershed (Sufrat Dishshah) not under the influence of the mountainous semi-arid climate. Three main phases of aggradation and three phases of downcutting have been observed. The first phase of aggradation occurred between 26,500 cal. BP and 11,300 cal. BP and has been attested to several phases of alluvial accumulation between the MIS 2 and the beginning of the Holocene Humid Period, so likely during an arid period.

The second phase of alluvial aggradation occurred towards the end of the Holocene Humid Period, between 6,200 cal. BP and 5,500 cal. BP. This data contributed to the ongoing discussion about the various proposed dates for the end of the Holocene Pluvial Period and highlighted the considerable potential of fluvial archives to address current gaps in understanding late quaternary climatic fluctuations and its local impact on specific environment. Cross-referencing hydro-climatic data of the Wadi Dishshah with the distribution of the archaeological sites from the Early and Middle Bronze Age in the Salakh Arch area reveals a late reorganization of sites after arid conditions began impacting surface flows, suggesting a delay either in the adaptative strategy of societies and/or in the environmental response to aridification.

A late torrential aggradation phase occurred around 2,800 cal. BP (during the Early Iron Age) while arid climate is already established. The downcutting phases have been correlated more with rainfall variability (fluvial dynamics and transport capacity) than with tectonic factors which are still poorly understood during the late Quaternary in this region. The aggradation phases are not clearly linked with humid periods identified in the speleothems, the study of the downstream part of Wadi Dishshah would help to better understand the possible asynchronous upstream-downstream reactions of the hydrosystem throughout its watershed.

Acknowledgements

The authors would like to acknowledge the Ministry of Heritage and Culture of the Sultanate of Oman for their support during the fieldwork, and especially Mr. Sultan al-Bakri. We would like also to thank the French Ministry of Foreign Affairs for its financial support through the program MEDEE (Mer, Désert et Environnement) directed by Pr. Eric Fouache. Our thanks go to the French Mission in Central Oman for their welcoming, logistics and financial support during each fieldwork. We would like to thank Raphaël Hautefort and Julien Guery from the Captair company for their work with the drone and support during the field campaigns and afterward. Last, we thank Dr. Louise Purdue and Pr. Gösta Hoffmann for their comments and suggestions to improve this paper. Finally, we would like to thank Dr. Lucas Proctor and Antoine Chabrol for their help in proofreading the English version.

References

Al-Khayat J.A. (2010) – First record of five terrestrial snails in the State of Qatar. Turkish Journal of Zoology, 34 (4), 539–545. DOI : 10.3906/zoo-0807-26

Amr M.Z., Al-Shammari A.M. (2013) – Terrestrial snails of Ha'il region, Saudi Arabia. International Journal of Current Science, 5, 1–5.

Balbo A.L., Gomez-Baggethun E., Salpeteur M., Puy A., Biagetti S., Scheffran J. (2016) – Resilience of small-scale societies: a view from drylands. Ecology and Society, 21 (2), Art. 53. DOI : 10.5751/ES-08327-210253

Béchennec F., Wyns R., Roger J., Le Métour J., Chevrel S. (1992) – Geological map of Nazwa and explanatory notes, scale 1:250,000, sheet NF 40-07, Sultanate of Oman. Ministry of Petroleum and Minerals, Directorate Generals of Minerals. BRGM.

Berger J.-F., Charpentier V., Crassard R., Martin C., Davtian G., Lopez-Saez J.A. (2013) – The dynamics of mangrove ecosystems, change in sea level and the strategies of Neolithic settlements along the coast of Oman (6,000-3,000 cal. BC). Journal of Archaeological Science, 40, 3087–3104. DOI : 10.1016/j.jas.2013.03.004

Berger J.-F., Bravard J.-P., Purdue L., Benoist A., Mouton M., Braemer F. (2012) – Rivers of the Hadramawt watershed (Yemen): Clues for a late functioning. Quaternary International, 266, 142–161. DOI : 10.1016/j.quaint.2011.10.037

Beshkani A., Beuzen-Waller T., Bonilauri S., Gernez G. (2017) – The First Evidence of Nubian Technique in the Adam Region, Oman. Antiquity Project Gallery, 91 (356). DOI : 10.15184/aqy.2017.4

Beuzen-Waller T., Giraud J., Gernez G., Courault R., Kondo Y., Cable M.C., Thronton C. (2018) – L'émergence des territoires proto-oasiens dans les piémonts du Jebel Hajar. Approche géoarchéologique multicritère et comparative. Actes de colloque des XVIIIe rencontres internationales d'Archéologie et d'Histoire d'Antibes, 179–205.

Blechschmidt I., Matter A., Preusser F., Rieke-Zapp D. (2009) – Monsoon Triggered Formation of Quaternary Alluvial Megafans in the Interior of Oman. Geomorphology, 110 (3-4), 128–139. DOI : 10.1016/j.geomorph.2009.04.002

Bonilauri S., Beuzen-Waller T., Giraud J., Lemée M., Gernez G., Fouache E. (2015) – Occupation during the Lower and Middle/Late Palaeolithic period in the Sufrat Valley (Sultanate of Oman). Proceedings of the Seminar of Arabian Studies, 45, 1–14.

Breeze P.S., Groucutt H.S., Drake N.A., White T.S., Jennings R.P., Petraglia M.D. (2016) – Palaeohydrological corridors for hominin dispersals in the Middle East 250,000-70,000 years ago. Quaternary Science Reviews, 144, 155–185. DOI : 10.1016/j.quascirev.2016.05.012.

Charbonnier J. (2014) – In the shadow of the palm trees: time management and water allocation in the oasis of Ādam (Sultanate of Oman). Proceedings of the Seminar for Arabian Studies, 44, 83–98.

Clark I.D., Fontes J.–C. (1989) – Paleoclimatic Reconstruction in Northern Oman Based on carbonates from Hyperalkaline Ground-waters. Quaternary Research, 3, 320–336.

Cremaschi M., Degli Esposti M., Fleitmann D., Perego A., Sibilia E., Zerboni A. (2018) – Late Holocene Onset of Intensive Cultivation and Introduction of the Falaj Irrigation System in the Salut Oasis (Sultanate of Oman). Quaternary Science Reviews, 200, 213–240. DOI : 10.1016/j.quascirev.2018.09.029

Cremaschi M., Zerboni A., Charpentier V., Crassard R., Isola I., Regattieri E., Zanchetta G. (2015) – Early-Middle Holocene

environmental changes and pre-Neolithic human occupation as recorded in the cavities of Jebel Qara (Dhofar, southern Sultanate of Oman). Quaternary International, 382, 264–276.
DOI : 10.1016/j.quaint.2014.12.058

Desruelles S., Fouache E., Eddargach W., Cammas C., Wattez J., Beuzen-Waller T., Martin C., Tengberg M., Cable M.C., Thornton C., Murray A. (2016) – Evidence for Early Irrigation at Bat (Wadi Sharsah, Northwestern Oman) before the Advent of Farming Villages. Quaternary Science Reviews, 150, 42–54.
DOI : 10.1016/j.quascirev.2016.08.007

Engel M., Brückner H., Pint A., Wellbrock K., Ginau A., Voss P., Grottker M., Klasen N., Frenzel P. (2012) – The early Holocene humid period in NW Saudi Arabia – Sediments, microfossils and palaeo-hydrological modelling. Quaternary International, 266, 131–141.
DOI : 10.1016/j.quaint.2011.04.028

Fleitmann D., Matter A. (2009) - The speleothem record of climate variability in Southern Arabia. Comptes Rendus Geoscience, 341, 633–642.
DOI : 10.1016/j.crte.2009.01.006

Fleitmann, D., Burns, S.J., Pelaka, M., Mangini, A., Al-Subbary, A., Al-Aowah, M., Kramers, J., Matter, A. (2011) – Holocene and Pleistocene pluvial periods in Yemen, southern Arabia. Quaternary Research, 60, 223–232.
DOI : 10.1016/j.quascirev.2011.01.004

Fleitmann D., Burns S.J., Mangini A., Mudelsee M., Kramers J., Villa I., Neff U., Al-Subbary A.A., Buettner A., Hippler D., Matter A. (2007) – Holocene ITZC and Indian monsoon dynamics recorded in stalagmites from Oman and Yémen (Socotra). Quaternary Science Reviews, 26, 170–88.
DOI : 10.1016/j.quascirev.2006.04.012

Fleitmann D., Burns S.J., Neff U., Mangini A., Matter A. (2003) – Changing moisture sources over the last 330,000 years in Northern Oman from fluid incision evidence in speleothems. Quaternary Research, 60, 223–232.
DOI : 10.1016/S0033-5894(03)00086-3

Fuchs M., Buerkert A. (2008) – A 20 ka sediment record from the Hajar Mountain range in N-Oman, and its implication for detecting arid–humid periods on the southeastern Arabian Peninsula. Earth and Planetary sciences letters, 265, 546–558.
DOI : 10.1016/j.epsl.2007.10.050

Galbraith R., Green P. (1990) – Estimating the component ages in a finite mixture. Nuclear Tracks and Radiation Measurements, 17 (3), 197–206.
DOI : 10.1016/1359-0189(90)90035-V

Galbraith R., Roberts R., Laslett G., Yoshida H., Olley J. (1999) – Optical dating of single and multiple grains of quartz from Jinmium Rock Shelter, Northern Australia: Part I. Experimental design and statistical models. Archaeometry, 41, 339–364.
DOI : 10.1111/j.1475-4754.1999.tb00988.x

Gernez G., Giraud J. (2015) – Protohistoric graveyards in Adam (Oman). Preliminary report on the 2013 and 2014 seasons of the French Archaeological mission to Adam. Proceedings of the Seminar for Arabian Studies, 45, 107–122.

Giraud J. (2012) – Les espaces du passé : L'exemple du Ja'alan à la période Hafit. In Giraud J. et Gernez G. (Eds) : Aux marges de l'archéologie : hommage à Serge Cleuziou. Travaux de la maison René-Ginouvès, 16, 133–151.

Giraud J., Gernez G. (2016) – The new funerary landscape during the beginning of the Early Bronze Age in Adam, Jabal Salakh and Jabal Qarah. In Gernez G. et Giraud J. (Eds): At the margins of the desert, Adam oasis in the Prehistory of Oman, The archaeological Heritage of Oman. Vol. 3, Ministry of Heritage and Culture.

Hoffmann G., Rupprechter M., Rahn M., Preusser F. (2015) – Fluvio-Lacustrine Deposits Reveal Precipitation Pattern in SE Arabia during Early MIS 3. Quaternary International, 382, 145–153.
DOI : 10.1016/j.quaint.2014.10.053

Jean M., Pellegrino M. P., Beuzen-Waller T., Casteja V., Gernez G. (2021) – Monumental terraces, water-spring and thousands of copper artefacts: last campaign at Mudhmar East 3 (2017–2019), Seminar of the Arabian studies 2021 – online session (poster).
DOI : 10.13140/RG.2.2.18734.59207

Jorgensen D.G., Al Tikriti, W.Y. (2002) – A hydrologic and archaeologic study of climate change in Al Ain, United Arab Emirates. Global and Planetary Changes, 35, 37–49.
DOI : 10.1016/S0921-8181(02)00090-5

Khanam S., Kazmi Q.B., Iqbal F. (2020) – Local dispersal of land snail Zootecus insularis (Ehrenberg, 1831) (Gastropoda : Subulinidae) shells in mangroves of Karachi. Indian Journal of Geo Marine Sciences, 49 (12).
http://nopr.niscair.res.in/handle/123456789/55944

Kondo Y., Beuzen-Waller T., Miki T., Noguchi A., Desruelles S., Fouache E. (2014) – Geoarchaeological survey in the Wadi al-Kabir basin, Wilayat Ibri, Oman: preliminary report. Supplement to the proceeding of the Seminar for Arabian Studies, 44, 1–8.

Lanos P., Dufresne P. (2019) – ChronoModel version 2.0: Software for Chronological Modelling of Archaeological Data using Bayesian Statistics, 84 p.

Lemée M., Gernez G., Giraud J., Beuzen-Waller T., Fouache E. (2013) – Jabal al-Aluya: an inland Neolithic settlement of the late fifth millennium BC in the Ādam area, Sultanate of Oman. Proceedings of the Seminar for Arabian Studies, 43, 197–212.

Lézine A.-M. (2009) – Timing of Vegetation changes at the end of the Holocene Humid Period in Desert Areas at the northern edge of the Atlantic and Indian monsoon system. Comptes Rendus Géoscience, 341, 750-59.
DOI : 10.1016/j.crte.2009.01.001

Lézine A.-M., Ivory S.J., Braconnot P., Marti O. (2017) – Timing of the Southward Retreat of the ITCZ at the End of the Holocene Humid Period in Southern Arabia: Data-Model Comparison, Quaternary Science Reviews, 164, 68–76.
DOI : 10.1016/j.quascirev.2017.03.019

Matter A., Neubert E., Preusser F., Rosenberg T., Al-Wagdani K. (2015) – Palaeo-environmental implications derived from lake and sabkha deposits of the southern Rub' al-Khali, Saudi Arabia and Oman. Quaternary International, 382, 120–131.
DOI : 10.1016/j.quaint.2014.12.029

Mc Clure H. (1976) – Radiocarbon chronology of late Quaternary lakes in the Arabian Desert. Nature, 263, 755–756.

McLaren S.J., Al-Juaidi F., Bateman M.D., Millington A.C. (2008) – First evidence for episodic flooding events in the arid interior of central Saudi Arabia over the last 60 ka. Journal of Quaternary Science, 24, 198–207.

DOI : 10.1002/jqs.1199

Mery S. (2013) – The first oases in Eastern Arabia: society and craft technology, in the 3rd millennium BC at Hili, United Arab Emirates. Revue d'ethnoécologie, Le palmier-dattier, 4, 2– 17.
DOI : 10.4000/ethnoecologie.1631

Moraetis D., Mattern F., Scharf A., Frijia G., Kusky T.M., Yuan Y., El-Hussain I. (2018) – Neogene to Quaternary uplift history along the passive margin of the northeastern Arabian Peninsula, eastern Al Hajar Mountains, Oman. Quaternary Research, 90, 1–17.
DOI : 10.1017/qua.2018.51

Mueller D., Raith K., Bretzke K., Fülling A., Parker A.G., Parton A., Preston G.W., Jasim S., Yousif E., Preusser F. (2022) – Luminescence chronology of fluvial and aeolian deposits from the Emirate of Sharjah, UAE. Quaternary Research, 1–17.
DOI : 10.1017/qua.2022.51

Murray A.S., Wintle A.G. (2003) – The single aliquot regenerative dose protocol: potential for improvements in reliability. Radiation Measurements, 37 (4–5), 377–381.
DOI : 10.1016/S1350-4487(03)00053-2

Neubert E. (1998) – Annotated checklist of the terrestrial and freshwater molluscs of the Arabian Peninsula with descriptions of new species. Fauna of Arabia, 17, 333–462.

Parker A.G. (2009) – Pleistocene climate change in Arabia: developing a Framework for hominin dispersal over the last 350 ka. In Petraglia M. D. and Rose J. I. (Eds): The Evolution of Human population in Arabia. Palaeoenvironments, Prehistory and Genetics. Vertebrate Paleobiology and Paleoanthropology Series, Springer, 39–49.
DOI : 10.1007/978-90-481-2719-1_3

Parker A.G., Preston G.W., Parton A., Walkington H., Jardine P.E., Leng M.J., Hodson M.J. (2016) – Low latitude Holocene hydroclimate derived from lake sediment flux and geochemistry. Journal of Archaeological Science, 31 (4), 286–299.
DOI : 10.1002/jqs.2859

Parker A.G., Goudie A.S., Stokes S., White K., Hodson M.J., Manning M., Kennet D. (2006) – A record of Holocene climate change from lake geochemical analyses in southeastern Arabia. Quaternary Research, 66, 465-76.
DOI : 10.1016/j.yqres.2006.07.001

Parton A., White T.S., Parker A.G., Breeze P.S., Jennings R., Groucutt H.S., Petraglia M.D. (2015) – Orbital scale variability in Arabia as a potential motor for human dispersals. Quaternary International, 382, 82–97.
DOI : 10.1016/j.quaint.2015.01.005.

Parton A., Farrant A.R., Leng M.J., Schwenninger J.-L., Rose I. J., Uerpmann H.-P., Parker A.G. (2013) – An early MIS 3 pluvial phase in Southeast Arabia: climatic and archaeological implications. Quaternary International, 300, 62–74.
DOI : 10.1016/j.quaint.2013.02.016

Petraglia M.D., Groucutt H.S., Guagnin M., Breeze P.S., Boivin N. (2020) – Human responses to climate and ecosystem change in ancient Arabia. PNAS, 117 (15), 8263–270.
DOI : 10.1073/pnas.1920211117

Petraglia M.D., Parton A., Groucutt H.S., Alsharekh A.M. (2015) – Green Arabia: human prehistory at the crossroads of continents. Quaternary International, 382, 1–7.
DOI : 10.1016/j.quaint.2015.05.071

Pietsch D., Kühn P. (2012) – Early Holocene paleosols at the southwestern Ramlat As-Sab'atayn desert margin: New climate proxies for southern Arabia. Palaeogeography, Palaeoclimatology, Palaeoecology, 365-366, 154–165.
DOI : 10.1016/j.palaeo.2012.09.023

Pietsch D., Kühn P., Scholten T., Brunner U., Hitgen H., Gerlach I. (2010) – Holocene soils and sediments around Ma'rib Oasis, Yemen: Further Sabaean treasures? The Holocene, 20 (5), 785–799.
DOI : 10.1177/0959683610362814

Preston G.W., Parker A.G. (2013) – Understanding the evolution of the Holocene Pluvial Phase and its impact on Neolithic populations in south-east Arabia. Arabian archaeology and epigraphy, 24, 87–94.
DOI : 10.1111/aae.12006

Preston G.W., Thomas D.S.G., Goudie A. S., Atkinson O.A.C., Leng M.J., Hodson M.J., Walkington H., Charpentier V., Méry S., Borgi F., Parker A.G. (2015) – A multi proxy analysis of the Holocene humid phase from the United Arab Emirates and its implication for Southeast Arabia's Neolithic populations. Quaternary International, 382, 277–292.
DOI : 10.1016/j.quaint.2015.01.054

Preston G.W., Parker A.G., Walkington H., Leng M.J., Hodson M.J. (2012) – From nomadic herder-hunters to sedentary farmers: the relationship between climate change and ancient subsistence strategies in southeastern Arabia. Journal of Arid Environment, 86, 122–130.
DOI : 10.1016/j.jaridenv.2011.11.030

Purdue L., Kennet D., Garnier A., Parton A., Djerbi H., Botan S., Herveux L., Davtian G., Carré A., Moger D., al-Jahwari N. (2021) – Ancient agriculture in Southeast Arabia: A three thousand year record of runoff farming from central Oman (Rustaq). CATENA, 204, 105406.
DOI : 10.1016/j.catena.2021.105406

Purdue L., Charbonnier J., Régagnon E., Calastrenc C., Sagory T., Virmoux C., Crépy M., Costa S., Benoist A. (2019) – Geoarchaeology of Holocene oasis formation, hydro-agricultural management and climate change in Masafi, southern Arabia (UAE). Quaternary Research, 92, 109–132.
DOI : 10.1017/qua.2018.142

Radies D., Hasiotis S.T., Preusser F., Neubert E., Matter A. (2005) – Paleoclimatic significance of Early Holocene faunal assemblages in wet interdune deposits of the Wahiba Sand Sea, Sultanate of Oman. Journal of Arid Environments, 62 (1), 109–125.
DOI : 10.1016/j.jaridenv.2004.09.021

Reimer P., Austin W.E.N., Bard E., Bayliss A., Blackwell P.G., Bronk Ramsey C., Butzin M., Edwards R.L., Friedrich M., Grootes P.M., Guilderson T.P., Hajdas I., Heaton T.J., Hogg A., Kromer B., Manning S.W., Muscheler R., Palmer J.G., Pearson C., van der Plicht J., Richards D.A., Scott E. M., Southon J.R., Turney C.S.M., Wacker L., Adolphi F., Büntgen U., Fahrni S., Fogtmann-Schulz A., Friedrich R., Köhler P., Kudsk S., Miyake F., Olsen J., Sakamoto M., Sookdeo A., Talamo S. (2020) – The IntCal20 Northern Hemisphere radiocarbon age calibration curve (0–55 cal kB). Radiocarbon, 62 (4), 725–757.
DOI : 10.1017/RDC.2020.41.

Rose I.J., Hilbert Y. H., Marks A.E., Usik V. (2018) – Geography and Environment. The first people of Oman: Palaeolithic archaeology of the Nedj Plateau. Ministry of Heritage and Culture, Sultanate of Oman.

Rosenberg T., Preusser F., Blechschmidt I., Fleitmann D., Jagher R., Matter A. (2012) – Late Pleistocene palaeolake in the interior of Oman: a potential key area for the dispersal of anatomically modern humans out-of-Africa? Journal of Quaternary Science, 27, 13–16.
DOI : 10.1002/jqs.1560

Sanlaville P. (1992) – Changements climatiques dans la péninsule arabique durant le Pléistocène supérieur et l'Holocène. Paléorient, 18 (1), 5–26.

Searle M. (2019) – Geology of the Oman Mountains, Eastern Arabia, GeoGuide, Springer, 487 p.

Stuiver M., Reimer P.J. (1993) – Extended 14 C data base and revised CALIB.3.0. 14 C age calibration program. Radiocarbon, 35, 215–230.
DOI : 10.1017/S0033822200013904

Urban B., Buerkert A. (2009) – Palaeoecological analysis for Late Quaternary sediment profile in northern Oman. Journal of Arid Environment, 7, 296–305.
DOI : 10.1016/j.jaridenv.2008.09.023

Van Rampelbergh M., Fleitmann D., Verheyden S., Cheng H., Edwards L., De Geest P., De Vleeschouwer D., Burns S.J., Matter A., Claeys P., Keppens E. (2013) – Mid to Late Holocene Indian Ocean Monsoon Variability Recorded in Four Speleothems from Socotra Island, Yemen. Quaternary Science Reviews, 65, 129–142.
DOI : 10.1016/j.quascirev.2013.01.016

Version Française Abrégée

Au Sultanat d'Oman, les fluctuations climatiques quaternaires sont caractérisées par une alternance entre périodes humides et arides. La variabilité pluviométrique quaternaire est principalement contrôlée par la migration vers le nord de la Zone de Convergence Inter-Tropicale (ZCIT) et de la limite des moussons (Fleitmann et al., 2007). Durant les périodes humides du Pléistocène et de l'Holocène (Optimum climatique de l'Holocène : ~10 500 à 6 000 BP), les écoulements de surface sont plus réguliers, les points d'eau permanents plus nombreux, le couvert végétal mieux développé et les conditions arides qui prédominent actuellement au Sultanat d'Oman sont moins contraignantes. Ce sont donc des périodes favorables pour les chasseurs-cueilleurs du Paléolithique ; à l'Holocène, pour les groupes humains du Néolithique et éventuellement ceux de l'âge du Bronze ancien, période à laquelle la question de la gestion de la ressource en eau dans un contexte d'aridification croissante est régulièrement posée. Au Sultanat d'Oman, les formations alluviales sont encore peu étudiées malgré leur intérêt pour la reconstitution des réponses locales des hydro-systèmes aux fluctuations climatiques régionales. L'étude la plus aboutie est celle de Blechschmidt et al. (2009), ils démontrent que le forçage climatique prédomine dans la formation des terrasses alluviales au Pléistocène, que les périodes d'accumulation alluviale coïncident avec des périodes humides et les périodes d'incision avec des périodes arides. Dans cet article, nous étudions les formations alluviales héritées d'un petit wadi secondaire localisé à la marge du piémont sud du Jebel Hajar, dans le secteur de l'arche de Salekh : le Wadi Dishshah (fig. 1). Au nord du Sultanat d'Oman, cette étude est la première recherche publiée uniquement dédiée aux formations alluviales de la fin du Pléistocène et de l'Holocène. La cartographie précise d'un tronçon du Wadi Dishshah (fig. 3), l'étude morphostratigraphique de six coupes (fig. 4-6), leurs datations par radiocarbone ou OSL (tab. 1) et une étude malacologique ponctuelle (fig. 7) sont présentés. Cette étude a permis d'identifier trois générations de dépôts alluviaux, les accumulations de la première génération sont datées entre 26 500 cal. BP et 11 300 cal. BP, les dépôts de la deuxième génération entre 6 200 cal. BP et 5 500 cal. BP et une dernière phase d'accumulation est datée aux alentours de 2 800 cal. BP. Chaque génération a été incisée par des écoulements postérieurs qui ont taillé trois niveaux de terrasses (de la plus ancienne à la plus récente: T1, T2 et T3). La première génération de dépôts alluviaux (26 500 à 11 300 cal. BP) est surprenante car elle se situe durant une période classiquement considérée comme aride, mais elle coïncide une autre phase d'accumulation alluviale identifiée récemment aux Emirats arabes unis (Mueller et al., 2022). La deuxième génération de dépôts alluviaux se situe à la fin de la période humide de l'Optimum climatique de l'Holocène. L'étude géomorphologique, morphostratigraphique et malacologique a permis de reconstituer l'ajustement progressif du Wadi Dishshah et de son environnement proche à la réduction de la pluviométrie. Entre 6 500 cal. BP et 6 200 cal. BP, la plaine d'inondation du Wadi Dishshah est étendue. Jusqu'à 5 800 cal. BP, la partie distale de la plaine d'inondation est végétalisée et suffisamment humide pour permettre le développement de *Zootecus insularis* et *Pupoides coenopictus*. Entre 5 800 cal. BP et 5 500 cal. BP, le Wadi Dishshah migre vers le nord et la plaine d'inondation rétrécit ; la nappe alluviale TB est incisée par quelques paléochenaux qui sont colmatés à la fin de cette période. Cette étude démontre une réaction graduelle des hydro-systèmes à la réduction des précipitations à la fin de l'Optimum climatique de l'Holocène (fig. 8), datée dans cette partie du piémont du Jebel Hajar de la fin du Néolithique. Le dernier niveau d'accumulation (T3) présente 1,50 m de dépôts torrentiels. La seule date disponible indique une mise en place des dépôts vers de 2 800 cal. BP, soit durant l'âge du Fer. Des études géoarchéologiques récentes menées dans le secteur de l'arche de Salekh démontre le fonctionnement de sources, aujourd'hui taries, également à l'âge du Fer vers 2 730 à 2 460 cal. BP (Jean et al., 2021). D'autres études menées au Yémen et aux Emirats arabes unis (Berger et al., 2012 ; Purdue et al., 2019) indiquent une phase d'accumulation alluviale entre 2 800 et 2 200 BP, ce qui nous amène à nous interroger sur l'existence d'un possible épisode humide régional à l'âge du Fer. L'implication du facteur tectonique dans la formation des terrasses du Wadi Dishshah est également évoqué mais nos résultats et les données disponibles pour les taux de soulèvement au Quaternaire (Moraetis et al., 2018) ne permettent pas de pleinement évaluer l'influence de ce facteur.